NATIONAL SEMINAR 30th JANUARY, 2018

Abasaheb Marathe Arts & New Commerce, Science College,
Vikhare Gothane, Rajapur.
Dist: Ratnagiri (Maharashtra) India-416 702.
Phone: 02353-221002/ 221003
Fax: 02353-221003
E-mail: abasahebmarathecollege@gmail.com

ISBN No. 978-81-927211-2-8

Rayat Shikshan Sanstha's

Abasaheb Marathe

Arts & New Commerce, Science College,

Vikhare-Gothane, Rajapur. Dist- Ratnagiri (Maharashtra) 416 702

Proceedings

National Seminar on -

Emerging Trends in Basic Sciences,
Social Movements and Modern Development &
Management of Fruit Processing Industry in India

30th January, 2018

Organized by

Abasaheb Marathe
Arts & New Commerce, Science College,
In Association with
Internal Quality Assurance Cell (IQAC)

ISBN: 978-81-927211-2-8.

Rayat Shikshan Sanstha's

ABASAHEB MARATHE

ARTS AND NEW COMMERCE, SCIENCE COLLEGE, VIKHARE GOTHANE, RAJAPUR

Dist: Ratnagiri (Maharashtra) India-416 702.

Phone: 02353-221002/ 221003

Fax: 02353-221003

E-mail: abasahebmarathecollege@gmail.com

NAAC Reaccreditation: B (CGPA: 2.54)

One Day

National Seminar

On

"The Emerging Trends in Basic Sciences"

30th January 2018

Organized by

FACULTY OF SCIENCE

In association of

INTERNAL QUALITY ASSURANCE CELL (IQAC)

ABSTRACT BOOK &

PROCEEDINGS

CHIEF EDITOR

DR. SHAKIL. D. SHAIKH

Publisher: Prarup Publication, Karad

ISBN: 978-81-927211-2-8.

Publication Authority: I/c. Principal,
Dr. A. B. Tapase
Abasaheb Marathe Arts & New Commerce, Science College,
Vikhare Gothane, Rajapur.
Dist: Ratnagiri (Maharashtra) India-416 702.
Phone: 02353-221002/ 221003
Fax: 02353-221003
E-mail: abasahebmarathecollege@gmail.com

Chief Editor: Dr. Shakil Dilawar Shaikh
IQAC Co-ordinator, Head & Assistant Professor,
Department of Botany,
Abasaheb Marathe Arts and New Commerce, Science College,
Vikhare Gothane, Rajapur.
Dist: Ratnagiri (Maharashtra) India-416 702.
E-mail: lakish786@gmail.com
Mobile: 8805101469

Front Cover Design: Dr. Shakil Dilawar Shaikh

National Seminar

On

"The Emerging Trends in Basic Sciences"

30th January 2018

PROCEEDING

National Seminar on
"The Emerging Trends in Basic Sciences"
30th Jan, 2018

CONTENT

Study the effect of thickness on the structural, morphological and optical properties of Cu_2SnS_3 thin film prepared by CBD method

Harshad D. Shelke[a], Abhishek C. Lokhande[b], Vanita S. Raut[a], Chandrakant D. Lokhande[c]*
[a]Thin Film Physics Laboratory, Department of Physics, Shivaji University, Kolhapur-416 004 (M.S.), India.
[b]Optoelectronic Convergence Research Centre, Department of Materials Science and Engineering, Chonnam National University, Gwangju 500-757, South Korea
[a]A. M. A. and N. C. S. College, Rajapur, India
[c]Centre for Interdisciplinary Research, D. Y. Patil University, Kolhapur-416 006 (M.S.), India.
Corresponding author email; l_chandrakant@yahoo.com

Abstract

Cu_2SnS_3 (CTS) thin films of different thicknesses were prepared onto cost effective stainless steel substrate by chemical bath deposition method at the deposition temperature of 60^0C. X-ray diffraction pattern reveals that all the thin films prepared are polycrystalline in nature and crystallized in triclinic structure with preferential orientation along (2 -1 1) direction. The crystallite size increases from 34.12 nm to 53.30 nm with increase of film thickness. Morphology of the films as observed from the SEM indicates the presence of spherical particles. EDAX analysis shows that the films prepared are nearly stoichiometric without much deviation. From the optical spectra the nature of transition were found to be allowed and direct. The transmission of the film was found to decrease with increase of film thickness. The band gap energy decreased from 1.4 to 0.9 eV on increasing the film thickness. Photoelectrochemical (PEC) activity increased with increase of deposition time.

Keywords: Cu_2SnS_3, thin film, UV-vis, photoelectrochemical.

Introduction

With the energy crisis and environment problems becoming more and more serious, it is very urgent to explore new energy resource [1]. Solar energy is a promising new energy resource which is clean and sustainable. Cu–Sn–S, an important category of I-IV-VI chalcogenides functional materials, has attracted great attention because of their promising photocatalytic activity, photovoltaic property, nonlinear optical property, and outstanding optical-thermomechanical properties [2, 3]. Traditionally, these chalcogenides were prepared by solid-state reaction [4], which required high temperature, inert atmosphere protection, and a relatively long duration. The copper based multinary compound semiconductor materials are used as absorber materials in photovoltaic technology. Also, in recent years, importance is given to nontoxic semiconductors from both the fundamental and technological point of view for solar cell materials. Ternary semiconductors such as Cu-Sn-S belonging to I-IV-VI groups are preferred as excellent absorber material due to high absorption coefficient ($>10^4$ cm^{-1}) and small band gap (0.9 to 1.5 eV) for photovoltaic cells, and as a suitable candidate for nonlinear optical materials. In the Cu-Sn-S system, several ternary compounds including Cu_3SnS_3, Cu_2SnS_4, Cu_4SnS_4, $Cu_2Sn_3S_7$ and $Cu_4Sn_2S_7$ have been previously studied for photovoltaic absorbers. Among them, Cu_2SnS_3 (CTS) phase shows good performance in photovoltaic device because of its wide stability range and lack of Fermi level pinning [5]. Furthermore, this material offers outstanding optical, thermal and mechanical properties [6]. Various deposition methods have been used for preparing Cu–Sn–S compound thin films: successive ionic layer adsorption and reaction (SILAR) [7], sequential chemical deposition [8], solvothermal processing [9-11], solid-state reaction [12], spray pyrolysis [13], sputtering [14], chemical bath deposition (CBD) [15] and electrodeposition [16].

Among all these methods, the CBD method is very much famous because it possesses a number of advantages over predictable thin film deposition methods. The main advantages of this method are low cost, low deposition temperature and easy coating on the large surface area. This method is based on slow controlled precipitation of the preferred compound from its ions in a reaction bath solution. Therefore, we dedicated to develop a low-cost, facile, and environmental-friendly CBD method to synthesize I-IV-VI chalcogenides.

The characteristics of films and their potential applications are interrelated to the crystallinity, surface morphology, grain boundary and grain size, which are affected by the film thickness. For applications in optoelectronic devices technology, the optimum film thickness is

preferred for the best device quality and performance. Hence, it is necessary to study the effect of film thickness on the properties of CTS thin films. In present study, by varying the deposition time, thickness of CTS film is varied using optimized deposition condition and the effect of CTS film thickness on structural, morphological, wettability, optical and photoelectrochemical properties is studied.

2. Experimental procedure

2.1 Synthesis of CTS material

In a synthesis of CTS material, all chemicals used for the deposition process were analytical grade and all solutions were prepared in double distilled water (DDW). The deposition of CTS thin films onto commercial conducting stainless steel (SS) substrate. The SS substrates were polished by zero grade polish paper, ultrasonically cleaned in DDW for 5 minutes and then washed with acetone. The precursor solution was primed from an acidic bath using copper sulfate ($CuSO_4.5H_2O$), tin chloride ($SnCl_2.2H_2O$) and sodium thiosulfate ($Na_2S_2O_3.5H_2O$) acted as a source of copper, tin and sulfide ions, respectively. Ethylenediaminetetraacetic acid disodium salt (Na_2EDTA) is used as a complexing agent. The ratio of atomic weights is (2:1:3) for Cu:Sn:S in all deposition parameters. The solution of 0.2 M copper sulfate was dissolve into 20 ml of DDW and stirred until the clear solution is obtained. Then the solution of 0.1 M of stannous chloride was dissolved in 20 ml of DDW and was mixed into the as-prepared copper sulphate solution. 0.2 M of Na_2EDTA was dissolved in 10 ml of DDW and added to the above solution. The pH of the solution was attuned to1.5 by adding little drops of HCl (hydrochloric acid). Again the 20 ml of 0.3 M sodium thiosulfate was added into the above solution. The deposition process was carried out for 2h at 60 °C. Substrates were deep vertically in the solution bath. After deposition completion, the substrates covered by a material with desire thickness were washed by DDW to eliminate the contagion in the surface and annealed for 6h at 300 °C in a vacuum to pick up the crystallinity.

2.2 Materials characterization

The thickness of CTS films is measured by Ambios XP-1 surface profiler. The structural characterization of CTS nanoparticles is carried out using X-ray diffraction (XRD) by BRUKER AXS D8 Advanced model X-ray diffractometer equipped with Cu radiation (K_α of λ= 1.54 Å) operated at 40kV. Further confirmation of particular crystallographic phase is done from Raman spectroscopy were recorded in the range of 150–500 cm^{-1} by using a micro-Raman spectrometer (Via Reflex UV Raman microscope, Renishaw, U.K. at KBSI Gwangju center) that uses a He–Ne laser source. The morphological features of CTS nanoparticles are analyzed by scanning electron microscopy (SEM) JEOL JSM-6390. SEM technique is used to observe the grain size, rough morphology, and distribution of the particles on the surface of the system. The UV–visible optical absorption and transmittance spectra of CTS thin films have been carried out to explore their optical properties. The optical analysis carried out by a HITACHI UV4100 spectrometer in the wavelength ranging from 310 to 900 nm using cm^{-1} quartz cuvettes at room temperature. The current density-voltage (J-V) characteristics of the PEC cell were observed using a Princeton Applied Research Potentiostat (273A) with a CTS electrode as the working electrode.

3. Results and discussion

3.1 Thickness Measurement:

Fig. 1 shows the variation of film thickness with deposition time for CTS films is observed by CBD method. Thickness of CTS thin films is estimated to be 251, 420 and 590 nm for 60, 75 and 90 minutes deposition time, respectively. CBD deposited CTS thin films with 251, 420 and 590 nm thicknesses are indicated by **(a)** CTS-60, **(b)** CTS-75 and **(c)** CTS-90, respectively. It is observed that thickness of CTS film increases with deposition time. Ideally, in CBD method, only a single layer of film material is deposited on the substrate in one time of deposition. As the deposition times continue, more nucleation process is happened and more layers of the film material are deposited and hence the overall thickness of the film increases. This may be due to enough reaction time periods available for the formation of CTS thin film. The rate of film thickness is nonlinear which indicates that the growth is due to nucleation and coalescence process. Furthermore, after 90 minutes, slight decrease in CTS film thickness is observed. The reduction in CTS film thickness may due to the development of stress, resulting peel out the film

after reaching beyond optimum thickness. The peeling of film material is common in chemically deposited films and is mainly due to the relatively poor adhesion [17]. Thus, the terminal thickness of CTS thin film is 590 nm for 90 minutes deposition time.

3.2 Structural study

XRD pattern of CTS thin films prepared at different thicknesses are shown in **Fig. 2** (a-c). It is clear that the thickness plays an important role in determining the structure of the films. The film has polycrystalline nature with well-defined diffraction peaks, which can be well indexed to the triclinic crystal structure phase of CTS (JCPDS No.: - 00-027-0198). Li et al [18] represent the triclinic crystal structure of CTS material thin films. After enhancing the film thickness, all of the diffraction peaks are in good match with the standard pattern of triclinic CTS as shown in **Fig. 2**. The XRD patterns of CBD deposited CTS thin films with 251, 420 and 590 nm thicknesses are indicated by **(a)** CTS-60, **(b)** CTS-75 and **(c)** CTS-90, respectively in **Fig. 2**. The presence of peaks at 2θ = 28.49, 32.86 and 47.36 ^{0} corresponding to diffraction planes of (2 -1 1), (0 -4 2), (-2 0 10) and (-3 -2 10) respectively, indicates the formation of triclinic (JCPDS 00-027-0198) crystal structure of Cu_2SnS_3 material. The relative peak intensity of (2 1 1) and (-2 0 10) planes enhance with increasing film thickness. The enhanced crystallinity of the films can be attributed to the rearranging of the atoms and removal of defects due to the nucleation in CBD method. Manjulavalli et al. [19] reported the similar result of an increase in film crystallinity with increasing film thickness for CBD deposited CTS thin films. Apart from CTS XRD peaks, additional peak corresponding to secondary copper sulfate (CuS) phase (indicated by #) is observed in the diffraction pattern. The intensity of diffraction peaks increased after thickness increasing and became sharper. An additional peak at 2θ of 45.79° is observed after annealing, indicating the presence of minority secondary phase of Cu_2S. In annealed sample, secondary Cu_2S shows the single covellite phase with a hexagonal crystal structure and preferred orientation along the (102) direction. It is clear that the sample is multi-phase containing Cu_2S and Cu_2SnS_3 (JCPDS card no. 00-027-0198) with triclinic structure. The SS substrate peak in the XRD spectra is indicated by asterisk (*) sign. Crystalline grain size (D) of the films is evaluated using Scherrer formula,

$$D = \frac{K\lambda}{\beta Cos\theta} \quad (1)$$

Where, K is the shape factor, taken equal to 0.9, λ=1.54Å is the wavelength of the X-ray used, β is the full width at half maximum (FWHM) of the peak and θ is the Bragg angle that corresponds to the peak analyzed. The crystallite size of the films increased from 28 nm to 53 nm with increasing deposition time from 60 minutes to 90 minutes. The intensity of the peaks increases with increase of film thickness and full width half maximum (β) decreases, thereby leading to an increase in crystallite size. Structural parameters of CTS thin films were tabulated in **Table 1**. The result shows dislocation density and strain of the film decreases with increasing film thickness. Structural parameters of CTS thin films were tabulated in Table 1. The result shows dislocation density, strain and number of crystallites of the film decreases with increasing film thickness.

3.3 Energy dispersive X-ray analysis (EDAX)

The elemental study of the CTS thin films deposited at different deposition time on SS substrate are carried out by energy dispersive X-ray analysis (EDAX) technique. The respective EDAX spectra are shown in **Fig. 3** (a-c). EDAX examination implies the presence of copper, tin and sulfur for all the samples deposited at various deposition cycles. The stoichiometric ratio of Cu, Sn and S were determined by integrating the region under each Cu, Sn and S peak. Atomic percentage of Cu, Sn and S in CTS thin films for different thickness and the corresponding standard values are shown in **Table 2**. The chemical composition of the films presented in **Table 2** indicates the presence of Cu, Sn and S in stoichiometric amount with slightly copper rich content (Cu/Sn= 2.17-2.49). The film prepared at 45 minutes is found to be nearly same as that of standard value. It is also worth mentioning that the stoichiometric composition of the three film samples did not change significantly. EDAX spectrum also shows that prepared films are free from impurities.

3.4 SEM Analysis:

Fig. 3 (a-c) shows SEM images of CTS films with thickness of 251, 420 and 590 nm for 60, 75 and 90 minutes deposition time at 10,000X magnifications. An increasing deposition time show significant change in surface morphology of CTS thin films. Fig. 4 (a) shows a uniform distribution of spherically agglomerated nanocrystals i.e. it shows the complete crystal growth over the entire surface of substrate. It does not exhibit appreciable grain formation. The grain formation is seen in Fig. 4 (b). The uniform density, adhesion to the substrate and compact nature of the film increased with film thickness. With increase in deposition time, enhancement is agglomeration of the grains and compactness of the film, results in the formation of cluster type structure. SEM images in Fig. 4 (c) indicate that CTS film is composed of a dense packing of spherical grains without any voids, signifying uniformity and compact nature of thin film surface. It is observed that all the films are homogeneous and have dense microstructures. The film surface looks smooth and uniform. It is well clear from the micrographs that the particles are spherical and adherent. It can be seen that these spherical grains are uniformly distributed to cover the surface of the substrate completely. From the micrographs it is observed that the size of the grain increased with increase in deposition time as evinced by the XRD spectra. Also, a small crystallites growth on compact surface is observed. Further with increase in deposition time, film surface becomes deteriorated and slight decrease in film thickness is observed. Jadhav et al. [20] has reported deterioration in films, while Salgam et al. [21] observed macroscopic defects such as voids and cracks on the surface of the film with thickness.

3.5 Surface wettability study:

The contact angle depends upon the chemical composition and the surface morphology of the semiconducting electrodes. In this study, the water contact angle is found to be 84.9, 81.8 and 57.9° for with increasing deposition time from 60 minutes to 90 minutes, respectively (see Fig. 5). From surface wettability study, it is observed that the interfacial energy between the film surface and water increased with thickness leads to decrease in contact angle. Surface wettability is decreased with increase in film thickness due to two reasons: (a) thick film has relatively less internal and external strain energies compared to the thin one [22] and (b) the contact angle decreases with roughness of the film surface [23].

3.6 Optical Analysis:

The optical absorption of CTS thin films for different thicknesses has been investigated as shown in inset of Fig. 6 (a-c). The band gap energy of CTS thin films was calculated using the optical absorption spectroscopy. These spectra revealed that the deposited CTS thin films have high absorbance of light in the visible region, indicating its applicability as an absorbing material. Band gap values are estimated by plotting graph of $(\alpha h\upsilon)^2$ versus $(h\upsilon)$, where α is the absorption coefficient and $h\upsilon$ is the photon energy. The band gap (E_g) values are found to be 1.4, 1.2 and 0.9 eV for 60, 75 and 90 minutes deposition time, respectively. It is observed from Fig. 6, that the band gap gradually decreases from 1.4 to 0.9 eV with the increasing film thickness. The linear nature of the plots indicates the existence of the direct transitions. The decrease in band gap can be ascribed to the presence of secondary (CuS) phase in the compound as confirmed from the XRD study. Also from the compositional study, the Cu/Sn ratio increases from 2.17 to 2.49 with increasing film thickness. This increased copper composition results in absorbance of the light from the visible to IR region. Thus, the copper rich composition in the CTS compound leads to formation of secondary phase and eventually affects the band gap of the compound. Similar effect of band gap reduction from 1.4 to 0.9 eV for CTS films due to presence of secondary phases was observed by Zhao and Cheng [24].

3.7 Photo electrochemical (PEC) measurement:

Fig. 7 (a-c) shows the current-voltage (I-V) characteristics recorded under constant illumination conditions for CTS thin films of various thicknesses in 0.25 M $LiClO_4$ (Lithium perchlorate) electrolyte solution. The photovoltaic output characteristics of CTS thin films are studied by fabricating SS/CTS/$LiClO_4$/C Cell. Gradually increasing anodic photocurrent with increase in negative potential indicates p-type conductivity of CTS thin film [25]. The magnitude of short circuit current (I_{sc}) is 0.24, 0.35 and 0.50 mA and open circuit voltage (V_{oc}) is 35.20, 75 and 56 mV for various deposition time 60 to 90 minutes, respectively. The best PEC performance is obtained for 90 minutes deposition time thin film.

Solar cell parameters for CTS films of different thicknesses tabulated in **Table 3** shows that sample 90 minutes deposition time having 590 nm thicknesses, represents better PEC performance. The highest values of photo conversion efficiency 0.14% with fill factor of 265 % are achieved by 90 minutes deposition thin film. As discussed earlier (**Fig. 4**), that the level of compact surface enhances slightly with the film thickness, which is useful for PEC properties. The PEC measurement confirmed good photoactivity of different thicknesses CTS thin films, prepared by simple CBD method. Furthermore, the conversion efficiency of such film can be considerably increased by thermal, chemical and (photo) electrochemical surface treatments **[26]**.

Conclusions:

In conclusion, CTS thin films have been successfully deposited by simple and inexpensive CBD method. The effect of CTS film thickness on the structural, morphological, optical and PEC properties of CTS thin film is studied. The XRD studies revealed that CTS exhibit nanocrystalline structure with triclinic phase. Also, additional peak corresponding to secondary CuS phase is observed in the diffraction pattern. Improvement in crystallinity of the films with increasing film thickness was observed. The chemical composition of the films shows the presence of Cu, Sn and S in stoichiometric amount with slightly copper rich content (Cu/Sn= 2.17-2.49). The morphological study revealed that uniform, density, spherical and compact nature of the films increased with increasing film thickness. Also, with increasing CTS film thickness, optical band gap reduced which is related to enhancement in the crystallite size and decrease in defect density of the film. The study of PEC properties confirms good photoactivity for sample 90 minutes deposition time having 590 nm thicknesses. Hence, it can be concluded that the film thickness plays an important role in performance of PEC cells and on the characteristic parameters of the films.

References

[1] Z. Su, K. Sun, Z. Han, F. Liu, Y. Lai, J. Li Y. Liu, J. Mater. Chem., 22 (2012) 16346–16352.
[2] Onoda M. Chen X.A. Sato A. and Wada H., Mat. Res. Bull., 35 (2000) 1563–1570.
[3] Li B. Xie Y. Huang J.X. and Qian Y.T., J. Solid State Chem., 153 (2000) 170–173.
[4] M. Bouaziz, M. Amlouk, S. Belgacem, Thin Solid Films, 517 (2009), 2527–2530.
[5] L. Baranowski, K. McLaughlin, P. Zawadzki, S. Lany, A. Norman, H. Hempel, R. Eichberger, T. Unold, E. Toberer and A. Zakutayev, Phys. Rev. Applied, 4 (2015) 044017(1)-044017(9).
[6] M. Adelifard, M. Mohagheghi, H. Eshghi, The Royal Swedish Acad. of Sci. Physica Scripta, 85 (2012) 035603-035608.
[7] T. Reddy, R. Amiruddin, M. Santhoshkumar, Sol. Energy Mater. Sol. Cells, 143 (2015) 128–134.
[8] Y. Miyata, S. Nakamura, Y. Akaki, Phys. Status Solidi (C), 12 (2015) 765–768.
[9] X. Chen, H. Wada, A. Sato, M. Mieno, J. Solid State Chem., 139 (1998) 144–151.
[10] R. Ettlinger, A. Cazzaniga, S. Canulescu, N. Pryds, J. Schou, Appl. Surf. Sci., 336 (2015) 385–390.
[11] S. Vanalakar, G. Agawane, A. Kamble, C. Hong, P. Patil, J. Kim, Sol. Energy Mater. Sol. Cells, 138 (2015) 1–8.
[12] M. Nakashima, J. Fujimoto, T. Yamaguchi, and M. Izaki, Appl. Phys Express., 8 (2015) 04ES08 (1)-04ES08 (6).
[13] A. Crovetto, R. Chen, R. Ettlinger, A. Cazzaniga, J. Schou, C. Persson and O. Hansen, Sol. Energy Mater. Sol. Cells, 154 (2016) 121–129.
[14] B. Taher, M. Alias, I. Naji, H. Alawadi, A. Douri, Aust. J. Basic appl. Sci., 9 (2015) 406-411.

[15] J. Han, Y. Zhou, Y. Tian, Z. Huang, X. Wang, J. Zhong, Z. Xia, B. Yong, H. Song and J. Tang, Front Optoelectron, 7 (2014) 37.

[16] M. Shawky, A. Shenouda, El. Said, I. Ibrahim, Int. J. Sci. Engg. Res., 6 (2015) 1447.

[17] R. Salunkhe, D. Dhawale, T. Gujar, C. Lokhande, Mater Res Bull., 46 (2009) 5009-5015.

[18] B. Li, Y. Xie, J. Hang, Y. Qian, J. Solid State Chem., 153 (2000) 170–173.

[19] T. Manjulavalli, A. Kannan, Int.J. ChemTech Res., 8(10) (2015) 259-265.

[20] U. Jadhav, S. Patel and R. Patil, Res. J. Mater. Sci. 1 (2013) 21–25.

[21] M. Saglam, A. Ateş, B. Guzeldir and O. Ozakın, Phys. Status Solidi (A), 209 (2012) 687–693.

[22] A. More, J. Gunjkar, C. Lokhande, R. Mane and S. Han, Micron, 38 (2007) 500–504.

[23] G. Palasantzas and J. Hosson, Acta Materialia, 49 (2001) 3533-3538.

[24] Zhao and Cheng, Adv. Mater. Sci. Eng., 203 (2013) 1–4.

[25] Y. Chen, C. Chuang, K. Lin, S. Shen, C. McCleese, L. Guo, C. Burda, J. Phys. Chem. C, 118 (2014) 11954−11963.

[26] D. Brion, Appl. Surf. Sci., 5 (1980) 133-152.

Figure Captions:

Fig. 1 Plot of thickness variation of (a) CTS-60, (b) CTS-75 and (c) CTS-90 CTS thin films.

Fig. 2 XRD patterns of (a) CTS-60, (b) CTS-75 and (c) CTS-90 CTS thin films.

Fig. 3 Energy dispersive X-ray spectroscopy (EDAX) of (a) CTS-60, (b) CTS-75 and (c) CTS-90 thin films.

Fig. 4 SEM images of (a) CTS-60, (b) CTS-75 and (c) CTS-90 thin films at 10,000X magnifications.

Fig. 5 Surface wettability analysis of (a) CTS-60, (b) CTS-75 and (c) CTS-90 thin films.

Fig. 6 Band gap plots and optical absorption spectra of (a) CTS-60, (b) CTS-75 and (c) CTS-90 thin films.

Fig. 7 Photovoltaic output characteristics of (a) CTS-60, (b) CTS-75 and (c) CTS-90 thin film.

Table caption:

Table 1 Structural parameters of CTS material.

Table 2 Atomic percentage of Cu, Sn and S in CTS thin films.

Table 3 Photoelectrochemical cell parameters of CTS materials.

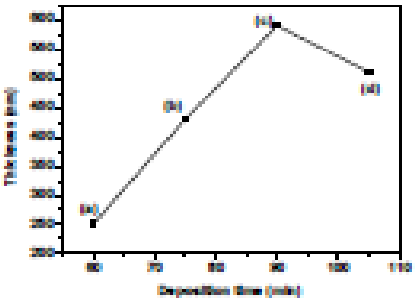

Fig. 1

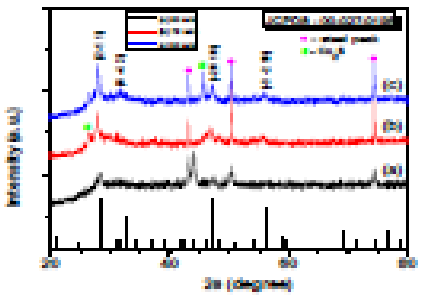

Fig. 2

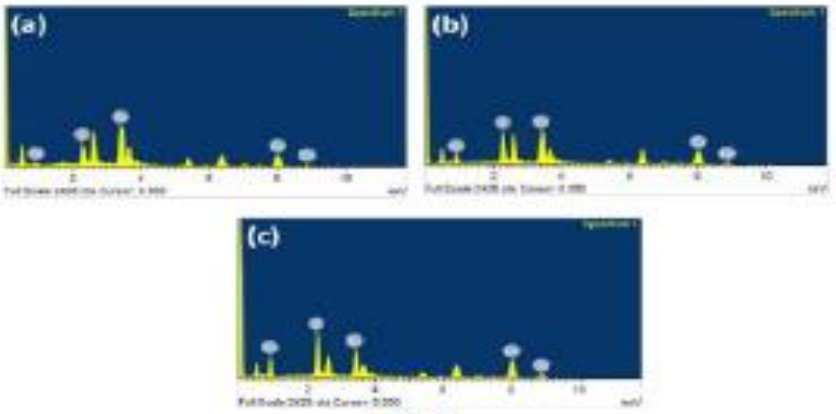

Fig. 3

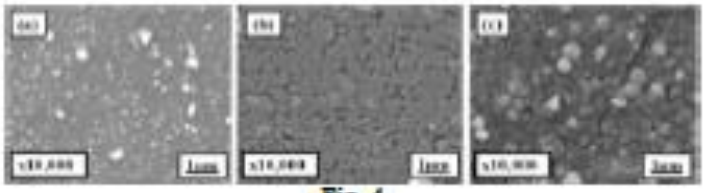

Fig. 4

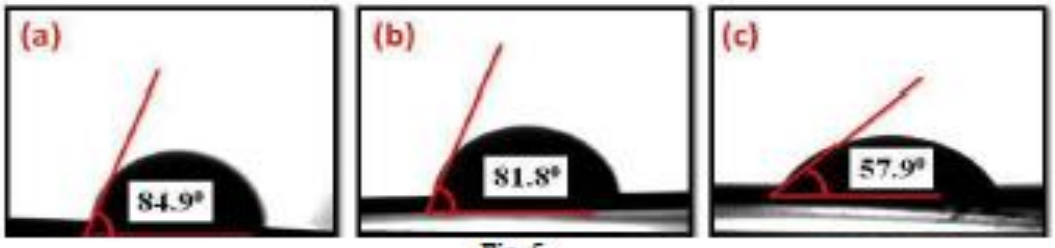

Fig. 5

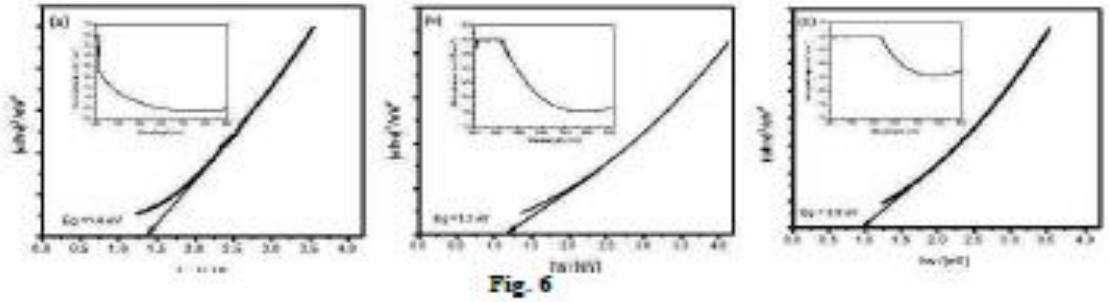

Fig. 6

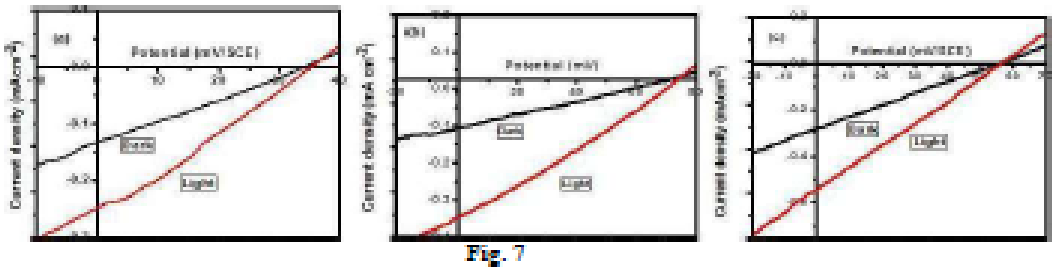

Fig. 7

Table 1

Deposition time (min)	Film thickness (nm)	hkl	Crystalline size D (nm)	Strain $\varepsilon \times 10^{-3}$ ($line^{-2}\ m^{-4}$)	Dislocation density $\delta \times 10^{-3}$ (nm^{-2})	$N \times 10^{17}$ (m^{-2})
60	251	(2 -1 1)	34.12	9.21	0.68	5.42
75	430	(2 -1 1)	42	8.25	0.56	4.21
90	590	(2 -1 1)	53.30	6.50	0.35	1.30

Table 2

Deposition time (min)	Standered			Calculated			Cu/Sn
	Cu at. %	Sn at. %	S at. %	Cu at. %	Sn at. %	S at. %	
60	33.33	16.67	50	29.31	13.5	54.79	2.17
75				30.40	13.1	56.5	2.32
90				31.71	12.7	57.99	2.49

Table 3

Deposition time (min)	Film thickness nm	I_{sc} (mA)	V_{oc} (mV)	I_m (mA)	V_m (mV)	FF %	Efficiency η %
60	251	0.24	35.20	0.15	15.66	0.277	0.004
75	430	0.35	75	0.21	30	0.241	0.126
90	590	0.50	56	0.31	24	0.265	0.145